

Vedran Mrzljak

E-mail: vedran.mrzljak@riteh.hr

Faculty of Engineering, University of Rijeka, Vukovarska 58, 51000 Rijeka, Croatia

Jan Kudláček

E-mail: jan.kudlacek@fs.cvut.cz

Czech Technical University of Prague, Zikova 1903/4, 166 36 Prague 6, Czech Republic

Đerzija Begić-Hajdarević

E-mail: begic@mef.unsa.ba

Faculty of Mechanical Engineering, University of Sarajevo, Vilsonovo šetalište 9,
71000 Sarajevo, Bosnia and Herzegovina

Jelena Musulin

E-mail: jmusulin@riteh.hr

Faculty of Engineering, University of Rijeka, Vukovarska 58, 51000 Rijeka, Croatia

The Leakage of Steam Mass Flow Rate through the Gland Seals – Influence on Turbine Produced Power

Abstract

In this paper is presented an analysis of gland seals operation and their influence on the performance of low power steam turbine with two cylinders and steam reheating, which can be used in marine applications. Performed analysis presents a comparison of steam turbine main operating parameters when gland seals operation is neglected (as usual in the most of the literature) and when steam mass flow rates leaked through all gland seals are taken into consideration. Steam mass flow rate leakage through all gland seals reduces produced power of the whole turbine and both of its cylinders. Operation of gland seal mounted at the inlet in the first cylinder of any steam turbine (cylinder which operates with the steam of the highest pressure) has the most notable influence on the reduction of the whole turbine produced power. Gland seal mounted at the outlet of the last turbine cylinder (cylinder which operates with the steam of the lowest pressure) did not have any influence on the reduction of steam turbine produced power. In any detail analysis of a steam turbine (especially the complex turbine with multiple cylinders), gland seals operation should be considered due to their notable influence on the turbine performance.

Keywords: Gland seals, Steam mass flow rate leakage, Steam turbine power

1. Introduction

Steam turbines are nowadays used in various power plants worldwide and can have many important functions [1].

In conventional power plants the base steam turbine units are composed of several cylinders (usually on the same shaft) which drive electrical generators [2-4]. Cumulative power produced in such turbines (by taking into account all the cylinders) is usually greater than 100 MW [5]. Therefore, such steam turbines are high power steam turbines.

Low power steam turbines have higher dispersion (in comparison to high power steam turbines) and can be used for many various functions than for the electrical generators drive only [6]. Low power steam turbines can be used in conventional power plants for the drive of several auxiliary plant power consumers [7]. Such turbines can also be found on various types of ships [8] where it can be used for ship propulsion [9] or for other ship requirements [10, 11]. In majority of ships with steam power plant, all the turbines inside such plants are low power steam turbines. The only exceptions can be found in army navy ships or submarines (large frigates, aircraft carriers, modern nuclear submarines, etc.) [12].

A literature review shows that, in the most of the cases, analyses of steam turbines (or the entire power plants) did not take into consideration labyrinth (gland) seals operation [13]. However, it is important to highlight that gland seals of each steam turbine cylinder significantly influenced cylinder and whole turbine operation [14], regardless of cumulative produced power. Steam mass flow rate leaked throughout each gland seal causes change in energy flow streams of the whole turbine and increases turbine power losses. Therefore, the operation of each gland seal inside one complex steam turbine should be taken into consideration in any detail analysis [15, 16].

In this paper are performed two analyses of complex, low power steam turbine with two cylinders, which can be used in several marine applications. In the first analysis, steam mass flow rate leakage through all gland seals is neglected - the turbine analysis is performed in the same way as usual in the literature. After that, in the second analysis, steam mass flow rate leakage throughout each gland seal is taken into consideration. It is presented and analyzed the influences of gland seals operation on energy flow streams of the observed turbine and on the turbine power losses. Both analyses are compared with an aim to get a proper insight into gland seals operation and their influences on reduction of steam turbine produced power.

2. Description and operating characteristics of the analyzed steam turbine

Analyzed steam turbine, which scheme and required operating points are presented in Figure 1, operates in a typical pulverized coal-fired steam power plant analyzed in [17]. Steam production in steam generator [18-20] of the observed power plant can be obtained by using various fuel types.

After its production in steam generator, superheated steam is delivered to the inlet of the observed turbine, Figure 1. Whole analyzed steam turbine consists of two cylinders (turbines) – High Pressure Turbine (HPT) and Low Pressure Turbine (LPT). Between steam turbine cylinders, is mounted reheater (RH) in which heat obtained by fuel combustion is used to increase steam temperature [21] before its expansion in LPT. At the observed power plant, a reheater is not independent component; it is mounted inside the steam generator similar to many other power plants [22, 23]. After expansion in LPT, remaining steam mass flow rate is delivered to the main steam condenser for condensation (saturated steam) [24, 25]. Both observed steam turbine cylinders are connected to the same shaft which drives an electrical generator (EG) [26]. The analyzed steam turbine has only one steam extraction (at the HPT outlet) which delivers a certain amount of steam to deaerator for feed water heating and deaerating purposes, Figure 1.

Each steam turbine cylinder (HPT and LPT) has two labyrinth (gland) seals (GS) mounted at each cylinder inlet and outlet (front and rear gland seals). One small part of the steam mass flow rate, which enter in each turbine cylinder did not expand through the cylinder stages, but leaked between cylinder rotor and its housing through front gland seal. After steam expansion in each cylinder, again one small part of the steam will leak between cylinder rotor and its housing through cylinder rear gland seal. The main function of each gland seal is to reduce leaked steam pressure. Leaked steam with decreased pressure will be delivered from each gland seal to gland steam (GS) condenser.

It is important to note that in the various analyses of steam power plants or steam turbines for itself, steam mass flow rate leakage through gland seals is not taken into consideration [27-30]. The analysis in this paper is performed firstly in the same manner – steam mass flow rate leakage through each gland seal is neglected. In the second part of this analysis – steam mass flow rate leakage through all gland seals is taken into consideration in order to obtain influences of each gland seal operation on the analyzed turbine energy flow streams and power losses.

The analyzed steam turbine is a low power turbine and it can also be used in various marine steam power plants which usually consist of such steam turbines (with or without reheating). In marine steam power plants, such turbine can be used not only for electrical generator drive, but also for the propulsion propeller drive (for example, on ships with steam propulsion) [31, 32]. The conclusions obtained in this paper about gland seals operation and their influences on the turbine energy flow streams and power losses will be valid regardless of the turbine usage origin (marine power plants or land-based power plants).

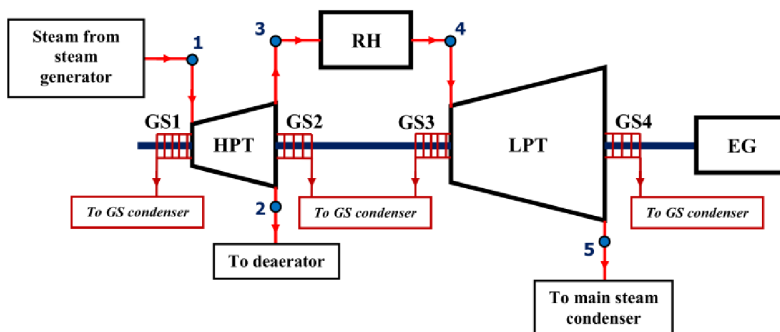


Figure 1: Steam turbine scheme and operating points required for the analysis

Steam expansion processes in each cylinder of the analyzed steam turbine (HPT and LPT) as well as the influence of the steam reheating process on turbine operation are presented in *h-s* diagram in Figure 2 (according to the turbine operating points from Figure 1). From Figure 2 can be observed that the steam mass flow rate extracted from the HPT (operating point 2) and steam mass flow rate delivered to reheater (operating point 3) has the same pressure and temperature and therefore the same specific enthalpy. Reheater has an important influence on the analyzed steam turbine process – it increases the steam temperature at the LPT inlet and increases steam content at the LPT outlet (main condenser inlet) in comparison with the process without reheating. Steam reheating process decreases the amount of water droplets inside steam at the last few LPT stages and at the main steam condenser inlet (LPT blades erosion in the last few stages will be significantly reduced which increases turbine operational time between major maintenances) [33].

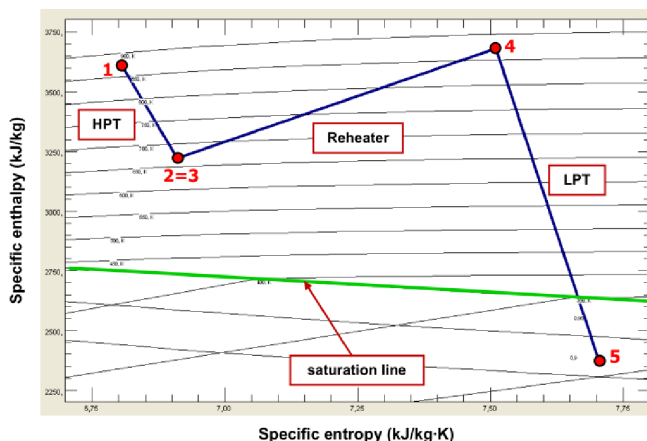


Figure 2: *h-s* diagram of steam expansion process inside observed steam turbine along with temperature increase in reheater

3. Equations and simplifications used in the analysis

The analysis in this paper is performed on the basis of energy and energy flow streams, which are based on the first law of thermodynamics [34, 35]. In comparison to other similar analysis [36-38] energy analysis did not take into consideration pressure and temperature of the ambient in which observed component or system operates [39-41].

The most important simplification in the presented analysis is neglecting all of the mechanical losses which occur inside the steam turbine and in the power transmission from turbine to power consumer. Such simplification is used in order to avoid all additional losses which occur in the analyzed turbine operation and to better highlight mass flow rate losses through all gland seals. All of the markings in the following equations are referring to Figure 1.

HPT produced power is calculated as:

$$P_{\text{HPT}} = \dot{m}_1 \cdot (h_1 - h_2) = \dot{m}_1 \cdot (h_1 - h_3), \quad (1)$$

while LPT produced power is calculated as:

$$P_{\text{LPT}} = \dot{m}_4 \cdot (h_4 - h_5). \quad (2)$$

Produced power of the whole observed turbine (WT) is the sum of produced power by HPT and LPT:

$$P_{\text{WT}} = P_{\text{HPT}} + P_{\text{LPT}} = \dot{m}_1 \cdot (h_1 - h_2) + \dot{m}_4 \cdot (h_4 - h_5). \quad (3)$$

Heat delivered to steam in reheater (heat is delivered by fuel combustion) is calculated as:

$$\dot{Q}_{\text{RH}} = \dot{m}_3 \cdot (h_4 - h_3). \quad (4)$$

Steam energy flow stream in each operating point of the observed steam turbine from Figure 1 is defined as can be found in [42, 43]:

$$\dot{E}_{\text{steam}} = \dot{m} \cdot h. \quad (5)$$

The same equations (from Eq. 1 to Eq. 5) are used in both analyses of observed steam turbine (without taking into consideration gland seals operation and by taking into consideration all gland seals operation). The differences between those two processes occurs in steam mass flow rates through each component (HPT, RH, LPT), according to steam mass flow rates leaked through gland seals. Steam temperatures and pressures in each operating point from Figure 1 remains the same for both analyses as well as

steam mass flow rate extracted from HPT (operating point 2, Figure 1).

In the analysis in which steam mass flow rates leaked through all gland seals are taken into consideration, it was important to calculate the power loss in the observed steam turbine caused by each gland seal. Steam mass flow rate leaked through each gland seal did not expand through the turbine and therefore reduces turbine produced power. However, each gland seal did not reduce turbine power identically. Each gland seal reduces turbine produced power similar as presented for turbine extractions in [44].

For the analyzed steam turbine, steam mass flow rate leaked through first gland seal (GS1) mounted at the HPT inlet, reduced produced power in both HPT and LPT. Turbine power loss caused by steam mass flow rate leakage through GS1 is:

$$Pl_{GS1} = \dot{m}_{GS1} \cdot (h_1 - h_2) + \dot{m}_{GS1} \cdot (h_4 - h_5). \quad (6)$$

Steam mass flow rate leaked through the second gland seal (GS2), which is mounted at the HPT outlet, reduced produced power in LPT and at the same time did not have influence on produced power in HPT. Turbine power loss caused by steam mass flow rate leakage through GS2 is:

$$Pl_{GS2} = \dot{m}_{GS2} \cdot (h_4 - h_5). \quad (7)$$

Steam mass flow rate leaked through the third gland seal (GS3), which is mounted at the LPT inlet, reduced produced power only in LPT. Turbine power loss caused by steam mass flow rate leakage through GS3 is:

$$Pl_{GS3} = \dot{m}_{GS3} \cdot (h_4 - h_5). \quad (8)$$

The last, fourth gland seal of the analyzed steam turbine (GS4) is mounted at the LPT outlet. Steam mass flow rate leaked through this gland seal did not have any influence on produced power in both HPT and LPT. Therefore, turbine power loss caused by steam mass flow rate leakage through GS4 is equal to zero:

$$Pl_{GS4} = 0. \quad (9)$$

In the above equations, P is produced power in kW, Pl is power loss in kW, \dot{Q} is heat delivered to steam in kW, \dot{E}_{steam} is steam energy flow stream in kW, \dot{m} is the steam mass flow rate in kg/s and h is steam specific enthalpy in kJ/kg.

4. Steam operating parameters of the observed turbine

Steam operating parameters (pressures, temperatures and mass flow rates) of the observed turbine, in each operating point from Figure 1, are found in [17] and

presented in Table 1. Steam operating parameters in Table 1 refers to power plant operation with bituminous coal. The authors in [17] did not take into consideration gland seals operation during its analysis, so the data from Table 1 is used in basic calculation performed in this paper. After the basic calculation, steam mass flow rate leaked through each gland seal was taken into consideration and it is investigated his influence on steam turbine operation.

Steam specific enthalpies, specific entropies and steam quality in each operating point from Table 1 are calculated by using NIST REFPROP 9.0 software [45]. It should be noted that in all operating points from Table 1 and Figure 1 steam is superheated, only in the last operating point, at the entrance in the main steam condenser (LPT outlet), the steam expansion process falls under the saturation line.

Table 1: Steam operating parameters in each required operating point of the analyzed turbine

Operating point*	Temperature (K)	Pressure (bar)	Mass flow rate (kg/s)	Specific enthalpy (kJ/kg)	Specific entropy (kJ/kg·K)	Steam quality
1	873.15	120	8.44	3608.9	6.8054	Superheated
2	669.05	30	2.35	3222.3	6.9095	Superheated
3	669.05	30	6.09	3222.3	6.9095	Superheated
4	873.15	30	6.09	3682.8	7.5103	Superheated
5	309.32	0.06	6.09	2373.4	7.7044	0.92

* Operating points refer to Figure 1.

Investigations of the steam turbine labyrinth (gland) seals operation are rare in the scientific and professional literature. Only in a few researches, characteristics and operation dynamics of steam turbine gland seals can be found. Cangioli et al. [46] presented thermo-elasto bulk-flow model for labyrinth seals in steam turbines, where the steam leakage through a labyrinth (gland) seals is investigated by using complex Computational Fluid Dynamics (CFD) simulations. Lorencin et al. [47] presented an exergy analysis of marine steam turbine labyrinth (gland) seals where the authors concluded that simplification of gland seals operation (by assuming the same steam specific enthalpy at each gland seal inlet and outlet) did not significantly differ in obtained results when compared to complex numerical models.

Kostyuk and Frolov [14] presented a numerical model for calculation of leaked steam mass flow rate through gland seals. The disadvantage of this model can be found in the fact that it involves several constants which do not have to be applicable in general, but the most important advantage is that the presented numerical model can be used as a good indicator of the leaked steam mass flow rate through each gland seal (numerical model also involves calculation of leaked steam mass flow rate through

each labyrinth seal inside the steam turbine). Blažević et al. [48] investigate various distributions of leaked steam mass flow rate through both gland seals (front and rear) of one steam turbine cylinder and its influence on the overall steam turbine energy analysis. Several important conclusions from [48] are also applied in the analysis performed in this paper.

In the analysis performed in this paper is assumed, as recommended in [48], that cumulative steam mass flow rate leaked through both gland seals of one steam turbine cylinder is equal to 1% of the steam mass flow rate at the cylinder inlet. Also, it is assumed that through each gland seal of one turbine cylinder leaked 50% of cumulative steam mass flow rate leaked in that cylinder. Those assumptions were applied in this paper for both analyzed steam turbine cylinders (HPT and LPT). According to recommendations from [48], this is the most common distribution of leaked steam mass flow rate through both gland seals of any steam turbine cylinder.

Therefore, in the second part of this analysis, when all gland seals operation is taken into consideration and according to steam mass flow rates from Table 1, leaked steam mass flow rate through each gland seal of the observed turbine is calculated and presented in Table 2. It should be noted that the steam mass flow rate leaked through first gland seal (GS1) has the same pressure and temperature as steam in operating point 1 from Figure 1, while the steam mass flow rate leaked through the second gland seal (GS2) has the same pressure and temperature as steam in operating point 2 and in operating point 3 from Figure 1. Also, the steam mass flow rate leaked through the third gland seal (GS3) has the same pressure and temperature as steam in operating point 4 from Figure 1, and finally, the steam mass flow rate leaked through the last fourth gland seal (GS4) of the analyzed turbine has the same pressure and temperature as steam in operating point 5 from Figure 1. Those elements are important in the calculation of steam energy flow streams throughout the observed turbine as well as in the calculation of turbine power losses caused by gland seals operation.

Table 2: Leaked steam mass flow rate through each gland seal of the analyzed turbine

Gland seal notation (according to Figure 1)	Leaked steam mass flow rate (kg/s)
GS1	0.0422
GS2	0.0422
GS3	0.0305
GS4	0.0305

5. Analysis results and discussion

5.1. Steam turbine analysis without taking into consideration gland seals operation

Produced steam turbine power (for each cylinder and the whole turbine) as well as heat delivered to steam in reheater for the analysis in which gland seals operation is not taken into consideration, are calculated by using data from Table 1 and equations from Eq. 1 to Eq. 4. The obtained results are presented in Figure 3.

Regardless of higher steam mass flow rate through HPT, due to significantly higher steam specific enthalpy drop, LPT produces much higher power (7974.25 kW) in comparison to HPT (3262.90 kW), while the whole turbine produced power, according to steam operating parameters from Table 1 is equal to 11237.15 kW, Figure 3. Heat delivered to steam in reheater is in this situation, when gland seals operation is not taken into consideration, equal to 2804.45 kW.

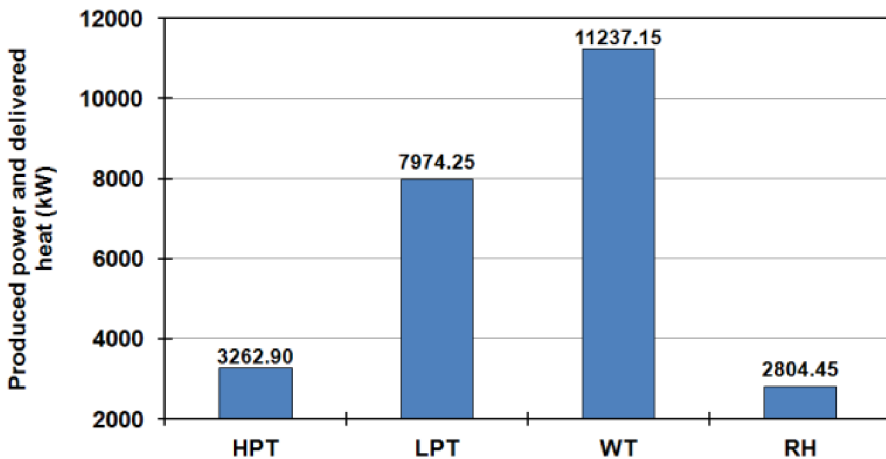


Figure 3: Produced power for the whole analyzed steam turbine and both of its cylinders as well as delivered heat in reheater, without taking into consideration gland seals operation

Steam energy flow streams and power throughout the entire analyzed turbine when gland seals operation is not taken into consideration (steam energy flow stream at the outlet of each gland seal is equal to 0 kW) are presented in Figure 4. Value of each steam energy flow stream is calculated according to operating parameters from Table 1, by using Eq. 5.

The highest steam energy flow stream is the one delivered from the steam generator (HPT inlet), equal to 30459.12 kW, which is then distributed through the turbine and used in each cylinder for power production. From Figure 4 can be concluded that the

deaerator in the observed power plant is significant steam consumer, because steam energy flow stream delivered to the deaerator (7572.41 kW) is approximately equal to one quarter of the steam energy flow stream at the HPT inlet. Steam energy flow stream delivered to the main condenser (LPT outlet) is in situation when turbine gland seals operation is not taken into consideration equal to 14454.01 kW, Figure 4. Cumulative EG driving power is the power produced in the whole steam turbine; it did not contain any mechanical losses during power transmission from steam turbine cylinders to an electrical generator.

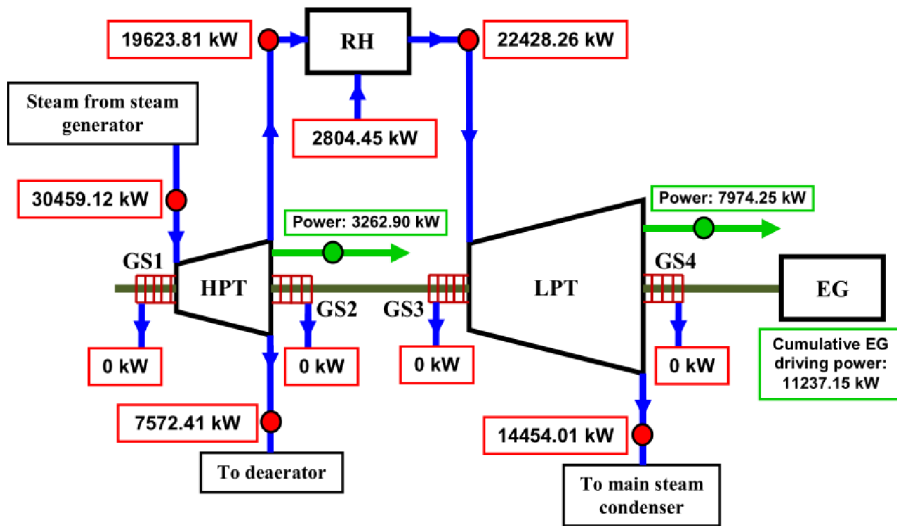


Figure 4: Steam energy flow streams and power throughout the analyzed turbine without taking into consideration gland seals operation

5.2. Steam turbine analysis by taking into consideration all gland seals operation

When operation and steam mass flow rate leakage in all gland seals of the observed steam turbine are taken into consideration (as described in the previous sections), the calculation of turbine power and delivered heat in the reheater are repeated, by using the equations from Eq. 1 to Eq. 4.

From the obtained results presented in Figure 5 can be seen that produced power of the whole steam turbine as well as of both its cylinders decreases in comparison to previous analysis when the gland seals operation is not taken into consideration. Also, the same comparison shows that heat delivered to steam in reheater also decreases, Figure 5. The decrease percentage for each component and the reasons of such decrease are further explained and discussed.

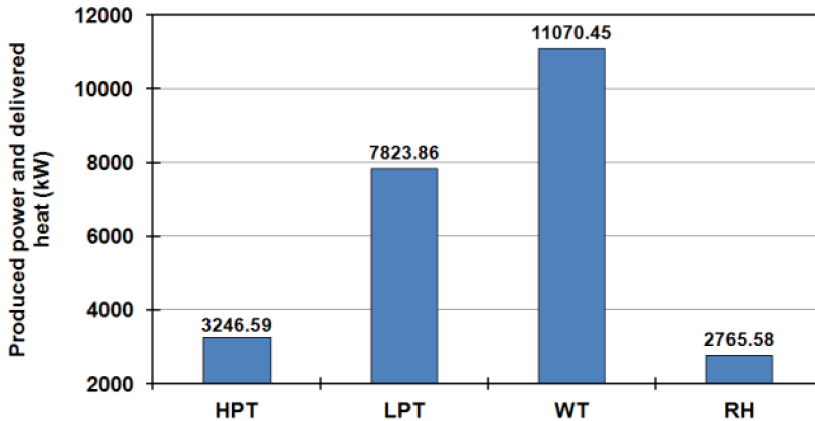


Figure 5: Produced power for the whole analyzed steam turbine and both of its cylinders as well as delivered heat in reheater, by taking into consideration all gland seals operation

Comparison of steam turbine operation without and with taking into consideration all gland seals operation show that gland seals operation reduced HPT produced power for 0.50%, Figure 6. The only reason for such reduction is the steam mass flow rate leaked through the first gland seal (GS1) which will not expand in HPT and will not participate in HPT produced power (in all operating points of Figure 1 steam pressures and temperatures remain the same). Steam mass flow rate leakage through GS2, mounted at the HPT outlet, did not participate in the HPT power reduction.

The gland seals operation causes produced power reduction of LPT for 1.89%, in comparison with the process when gland seals operation is not considered, Figure 6. It is important to note that the reduction of LPT produced power is much higher in comparison to HPT. By taking into account always the same steam mass flow rate extracted from the HPT (operating point 2, Figure 1), a steam mass flow rate which expands in LPT is reduced for steam leakage through three gland seals (GS1, GS2 and GS3). Therefore, due to the much higher reduction of the steam mass flow rate which expand in LPT (in comparison to HPT), LPT produced power is much more reduced than HPT produced power.

Reduction in produced power of the whole turbine, when gland seals operation is taken into consideration, is 1.48%. Such percentage of reduction in produced power for the whole turbine is much closer to the reduction of LPT produced power than to a reduction of HPT produced power because the majority of turbine power is produced in LPT.

Finally, heat delivered to steam in reheater is lower for 1.39% in the process when considering gland seals operation, Figure 6. The reason of such reduction in delivered heat is steam mass flow rate leakage through GS1 and GS2 what reduces the steam mass

flow rate which passes through the reheater. The lower amount of steam which passes through reheater (considering the same steam pressures and temperatures at reheater inlet and outlet as in the section 5.1) resulted with lower heat requirement. As the heat, which is delivered to steam in reheater, is produced by fuel combustion, lower amount of heat in reheater will reduce fuel consumption and harmful environmental emissions.

So, it can be concluded that operation of all gland seals will reduce produced power of the whole turbine (and both of its cylinders) - which is surely negative effect, but it will also reduce fuel consumption required for reheater operation - which is surely positive effect.

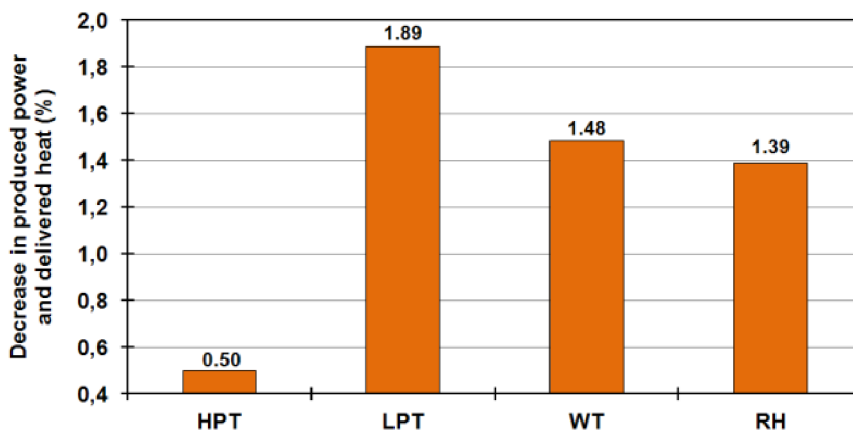


Figure 6: The percentage decrease in produced power for the whole analyzed steam turbine and both of its cylinders as well as the percentage decrease of heat delivered in reheater, by taking into consideration all gland seals operation

Turbine power loss caused by steam mass flow rate leakage through each gland seal is calculated by using equations from Eq. 6 to Eq. 9, and the obtained results are presented in Figure 7. Steam mass flow rate leakage through GS1 causes the highest power loss inside the observed steam turbine (71.571 kW) because this mass flow rate leakage reduces produced power of both turbine cylinders (HPT and LPT).

Steam mass flow rate leaked through the second (GS2) and third (GS3) gland seal causes power loss of LPT only (power loss in HPT is defined only by GS1 operation). A turbine power loss which is a result of GS2 operation is higher than power loss caused by GS3 operation due to higher value of mass flow rate leaked through GS2, Table 2.

The last, fourth gland seal (GS4) did not reduce turbine produced power, because steam after expansion in LPT is sent to main condenser and is not used anywhere else in the analyzed turbine. Steam after expansion in LPT has pressure significantly lower than the ambient one (condenser pressure, Table 1), so the main function of GS4 is to prevent air entry from the atmosphere into the LPT.

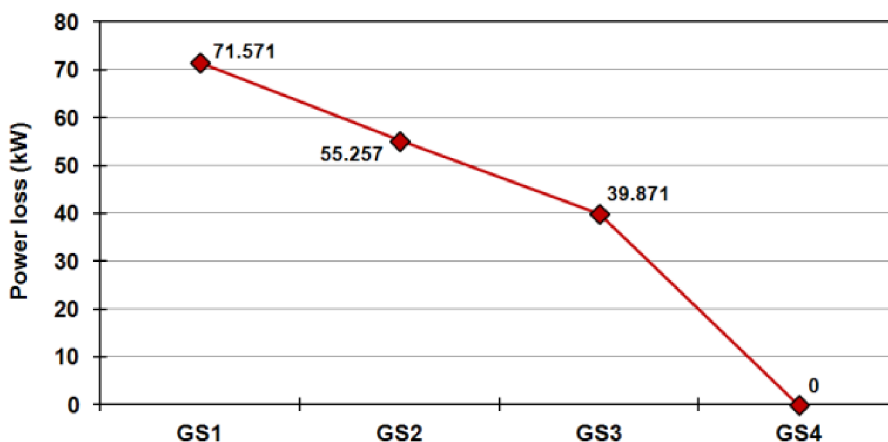


Figure 7: Power loss in the observed steam turbine caused by a steam mass flow rate leakage through each gland seal

Steam energy flow streams and power throughout the analyzed turbine by taking into consideration all gland seals operation are presented in Figure 8. In comparison with Figure 4 (where the gland seals operation is not considered), the gland seals operation reduced produced power in both turbine cylinders (reduction in produced power of HPT is equal to 16.31 kW, while reduction in produced power of LPT is equal to 150.39 kW), so the cumulative power which can be used for electrical generator drive is 11070.45 kW (mechanical losses during power transmission from steam turbine cylinders to electrical generator are again not taken into account). Due to lower steam mass flow rate through reheater, heat delivered by fuel combustion to steam in reheater is lower for 38.87 kW when gland seals operation is taken into consideration.

Steam mass flow rate leaked through GS1 has the highest pressure and temperature (in comparison to other gland seals), so steam energy flow stream delivered from GS1 to GS condenser is the highest and equal to 152.30 kW, Figure 8. Mass flow rates leaked through GS1 and GS2 are the same, but after the expansion in HPT steam has lower temperature and pressure than at the HPT entrance, so steam energy flow stream delivered from GS2 to GS condenser is lower in comparison with GS1 and equal to 135.98 kW. The same principle is valid for LPT, where steam energy flow stream delivered to GS condenser is higher for GS3 at the LPT inlet when compared to GS4 at the LPT outlet (112.14 kW in comparison to 72.27 kW).

From Figure 8 can be concluded that steam energy flow stream delivered to GS condenser is the highest for the first gland seal (at the turbine inlet, where the pressure is the highest) and then continuously decrease with a decrease in steam pressure until the turbine outlet.

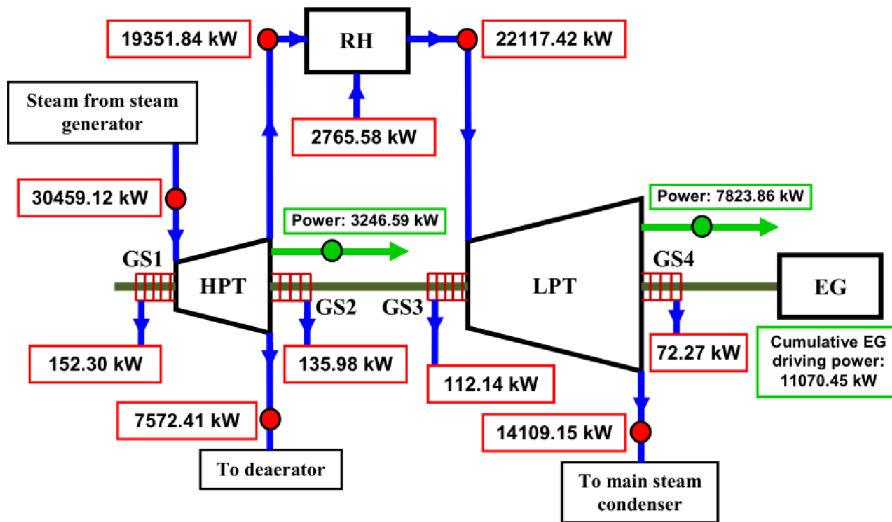


Figure 8: Steam energy flow streams and power throughout the analyzed turbine by taking into consideration all gland seals operation

Future research of presented steam turbine and its gland seals will firstly require much detailed measured data from exploitation (along with measurements of steam mass flow rates leaked through each gland seal) at various turbine loads. After obtaining such measured dataset, it will be used modern Artificial Intelligence (AI) tools [49-51] for further analyzing and possible optimizing [52, 53] observed steam turbine (and its gland seals) operation.

6. Conclusions

This paper presents an analysis of steam mass flow rate leakage through the turbine gland seals and their influence on the turbine produced power. The analyzed steam turbine is low power turbine with two cylinders and steam reheating. Such turbine can be used not only in conventional land-based but also in marine steam power plants. In this analysis is performed calculation of steam flow streams throughout analyzed turbine, turbine developed power and losses in two different cases - when gland seals operation is neglected and when gland seals operation is taken into consideration. Comparison of these two cases highlighted the most important conclusions of performed analysis, which are:

Steam mass flow rate leakage through turbine gland seals reduce produced power of the whole turbine and both of its cylinders.

Gland seals operation also reduces fuel consumption required for reheater operation, due to the lower steam mass flow rate through reheater (for obtaining the

same steam temperature at the reheater outlet).

Gland seal at the steam turbine inlet, which operates with the highest steam pressure, causes the most notable reduction in turbine produced power; because the steam mass flow rate leaked through this gland seal reduce produced power in all turbine cylinders. The influence of other gland seals on the reduction of turbine produced power is as lower as seal operates with the lower steam pressure.

The last gland seal (mounted at the outlet of the last turbine cylinder) did not have any influence on the reduction of steam turbine produced power.

Steam energy flow streams delivered from each gland seal to gland steam condenser are as higher as gland seal operates with higher steam pressure.

Decrease of steam mass flow rate leaked through gland seal mounted on the inlet into the turbine (the first gland seal) will have the highest influence on the reduction of turbine power losses.

In any detail analysis of steam turbine (especially the complex turbine with multiple cylinders), gland seals operation should be considered in detail, because, as presented in this paper - their operation has notable influence on the whole steam turbine performance.

Acknowledgments

This research has been supported by the Croatian Science Foundation under the project IP-2018-01-3739, CEEPUS network CIII-HR-0108, European Regional Development Fund under the grant KK.01.1.1.01.0009 (DATACROSS), University of Rijeka scientific grant uniri-tehnic-18-275-1447 and University of Rijeka scientific grant uniri-tehnic-18-18-1146.

References

1. Woodruff, E., Lammers, H. & Lammers, T. (2004). *Steam Plant Operation*. 8th edition. McGraw-Hill Professional.
2. Adibhatla, S. & Kaushik, S. C. (2014). Energy and exergy analysis of a super critical thermal power plant at various load conditions under constant and pure sliding pressure operation. *Applied Thermal Engineering*, 73, pp. 49-63. (doi:10.1016/j.applthermaleng.2014.07.030)
3. Erdem, H. H., Akkaya, A. V., Cetin, B., Dagdas, A., Sevilgen, S. H., Sahin, B., Teke, I., Gungor, C. & Atas, S. (2009). Comparative energetic and exergetic performance analyses for coal-fired thermal power plants in Turkey. *International Journal of Thermal Sciences*, 48, pp. 2179–2186. (doi:10.1016/j.ijthermalsci.2009.03.007)
4. Si, N., Zhao, Z., Su, S., Han, P., Sun, Z., Xu, J., Cui, X., Hu, S., Wang, Y., Jiang, L., Zhou, Y., Chen, G. & Xiang, J. (2017). Exergy analysis of a 1000 MW double reheat ultra-supercritical power plant. *Energy Conversion and Management*, 147, pp. 155–165. (doi:10.1016/j.enconman.2017.05.045)
5. Mitrović, D., Živković, D. & Laković, M. S. (2010). Energy and Exergy Analysis of a 348.5 MW Steam Power Plant. *Energy Sources, Part A*(32), pp. 1016–1027. (doi:10.1080/15567030903097012)
6. Hafidhi, F., Khir, T., Ben Yahyia, A. & Ben Brahim, A. (2015). Energetic and exergetic analysis of a steam turbine power plant in an existing phosphoric acid factory. *Energy Conversion and Management*, 106, pp. 1230-1241. (doi:10.1016/j.enconman.2015.10.044)
7. Adibhatla, S. & Kaushik, S. C. (2017). Energy, exergy, economic and environmental (4E)

- analyses of a conceptual solar aided coal fired 500 MWe thermal power plant with thermal energy storage option. *Sustainable Energy Technologies and Assessments*, 21, pp. 89–99. (doi:10.1016/j.seta.2017.05.002)
8. Mrzljak, V. & Mrakovčić, T. (2016). Comparison of COGES and diesel-electric ship propulsion systems. *Journal of Maritime & Transportation Sciences*, Special edition No. 1, pp. 131–148. (doi:10.18048/2016-00.131)
 9. Taylor, D. A. (1998). *Introduction to Marine Engineering*. Elsevier Butterworth-Heinemann.
 10. Mrzljak, V., Poljak, I. & Mrakovčić, T. (2017). Energy and exergy analysis of the turbo-generators and steam turbine for the main feed water pump drive on LNG carrier. *Energy Conversion and Management*, 140, pp. 307–323. (doi:10.1016/j.enconman.2017.03.007)
 11. McGeorge, H. D. (1995). *Marine Auxiliary Machinery*. 7th edition, Elsevier Science Ltd.
 12. Piwowarski, M. (2014). The Analysis of Turbine Propulsion Systems in Nuclear Submarines. *Key Engineering Materials*, 597, pp. 99–105. (doi:10.4028/www.scientific.net/kem.597.99)
 13. Noroozian, A., Mohammadi, A., Bidi, M. & Ahmadi, M. H. (2017). Energy, exergy and economic analyses of a novel system to recover waste heat and water in steam power plants. *Energy Conversion and Management*, 144, pp. 351–360. (doi:10.1016/j.enconman.2017.04.067)
 14. Kostyuk, A. & Frolov, V. (1988). *Steam and gas turbines*. Mir Publishers.
 15. Moran, M., Shapiro, H., Boettner, D. D. & Bailey, M. B. (2011). *Fundamentals of engineering thermodynamics*. 7th edition. John Wiley and Sons, Inc.
 16. McBirnie, S. C. (1980). *Marine Steam Engines and Turbines*. 4th Edition. Butterworth & Co. Ltd.
 17. Mehmood, S., Reddy, B. V. & Rosen, M. A. (2015) Exergy Analysis of a Biomass Co-Firing Based Pulverized Coal Power Generation System. *International Journal of Green Energy*, 12 (5), pp. 461–478. (doi:10.1080/15435075.2013.840834)
 18. Wang, C. & Zhu, Y. (2018). Entransy analysis on boiler air pre-heater with multi-stage LHS unit. *Applied Thermal Engineering*, 130, pp. 1139–1146. (doi:10.1016/j.applthermaleng.2017.11.085)
 19. Mrzljak, V., Poljak, I. & Medica-Viola, V. (2017). Dual fuel consumption and efficiency of marine steam generators for the propulsion of LNG carrier. *Applied Thermal Engineering*, 119, pp. 331–346. (doi:10.1016/j.applthermaleng.2017.03.078)
 20. Hajebzadeh, H., Ansari, A. N. M. & Niazi, S. (2019). Mathematical modeling and validation of a 320 MW tangentially fired boiler: A case study. *Applied Thermal Engineering*, 146, pp. 232–242. (doi:10.1016/j.applthermaleng.2018.09.102)
 21. Koroglu, T. & Sogut, O. S. (2018). Conventional and Advanced Exergy Analyses of a Marine Steam Power Plant. *Energy*, 163, pp. 392–403. (doi:10.1016/j.energy.2018.08.119)
 22. Kowalczyk, T., Ziolkowski, P. & Badur, J. (2015). Exergy Losses in the Szewalski Binary Vapor Cycle. *Entropy*, 17, pp. 7242–7265. (doi:10.3390/e17107242)
 23. Catrini, P., Cipollina, A., Micale, G., Piacentino, A. & Tamburini, A. (2017). Exergy analysis and thermoeconomic cost accounting of a Combined Heat and Power steam cycle integrated with a Multi Effect Distillation-Thermal Vapour Compression desalination plant. *Energy Conversion and Management*, 149, pp. 950–965. (doi:10.1016/j.enconman.2017.04.032)
 24. Laskowski, R. (2016). Relations for steam power plant condenser performance in off-design conditions in the function of inlet parameters and those relevant in reference conditions. *Applied Thermal Engineering*, 103, pp. 528–536. (doi:10.1016/j.applthermaleng.2016.04.127)
 25. Medica-Viola, V., Pavković, B. & Mrzljak, V. (2018). Numerical model for on-condition monitoring of condenser in coal-fired power plants. *International Journal of Heat and Mass Transfer*, 117, pp. 912–923. (doi:10.1016/j.ijheatmasstransfer.2017.10.047)
 26. Kumar, S., Kumar, D., Memon, R. A., Wassan, M. A. & Ali, M. S. (2018). Energy and Exergy Analysis of a Coal Fired Power Plant. *Mehran University Research Journal of Engineering & Technology*, 37 (4), pp. 611–624. (doi:10.22581/muet1982.1804.13)
 27. Ahmadi, G. R. & Toghraie, D. (2016). Energy and exergy analysis of Montazeri Steam Power Plant in Iran. *Renewable and Sustainable Energy Reviews*, 56, pp. 454–463. (doi:10.1016/j.rser.2015.11.074)
 28. Naserbegi, A., Aghaie, M., Minucmehr, A. & Alahyarizadeh, Gh. (2018). A novel exergy optimization of Bushehr nuclear power plant by gravitational search algorithm (GSA). *Energy*, 148, pp. 373–385. (doi:10.1016/j.energy.2018.01.119)
 29. Mrzljak, V. (2018). Low power steam turbine energy efficiency and losses during the developed power variation. *Technical Journal*, 12 (3), pp. 174–180. (doi:10.31803/tg-20180201002943)

30. Zhao, Z., Su, S., Si, N., Hu, S., Wang, Y., Xu, J., Jiang, L., Chen, G. & Xiang, J. (2017). Exergy analysis of the turbine system in a 1000 MW double reheat ultra-supercritical power plant. *Energy*, 119, pp. 540-548. (doi:10.1016/j.energy.2016.12.072)
31. Fernández, I. A., Gómez, M. R., Gómez, J. R. & Insua, A. A. B. (2017) Review of propulsion systems on LNG carriers. *Renewable and Sustainable Energy Reviews*, 67, pp. 1395–1411. (doi:10.1016/j.rser.2016.09.095)
32. Ammar, N. R. (2019). Environmental and cost-effectiveness comparison of dual fuel propulsion options for emissions reduction onboard LNG carriers. *Shipbuilding*, 70 (3), pp. 61-77. (doi:10.21278/brod70304)
33. Sutton, I. (2015). *Plant Design and Operations*. Elsevier Inc.
34. Kanoğlu, M., Çengel, Y. A. & Dincer, I. (2012). Efficiency Evaluation of Energy Systems. Springer Briefs in Energy. (doi:10.1007/978-1-4614-2242-6)
35. Mrzljak, V., Blecich, P., Anđelić, N. & Lorencin, I. (2019) Energy and Exergy Analyses of Forced Draft Fan for Marine Steam Propulsion System during Load Change. *Journal of Marine Science and Engineering*, 7 (11), 381. (doi:10.3390/jmse7110381)
36. Uysal, C., Kurt, H. & Kwak H.-Y. (2017). Exergetic and thermoeconomic analyses of a coal-fired power plant. *International Journal of Thermal Sciences*, 117, pp. 106-120. (doi:10.1016/j.ijthermalsci.2017.03.010)
37. Mrzljak, V., Poljak, I. & Žarković, B. (2018). Exergy Analysis of Steam Pressure Reduction Valve in Marine Propulsion Plant on Conventional LNG Carrier. *International Journal of Maritime Science & Technology "Our Sea"*, 65 (1), pp. 24-31. (doi:10.17818/NM/2018/1.4)
38. Mrzljak, V., Senčić, T. & Žarković, B. (2018). Turbogenerator Steam Turbine Variation in Developed Power: Analysis of Exergy Efficiency and Exergy Destruction Change. *Modelling and Simulation in Engineering*, 12 p. (doi:10.1155/2018/2945325)
39. Behrendt, C. & Stoyanov, R. (2018). Operational characteristic of selected marine turbomachines powered by steam from auxiliary oil-fired boilers. *New Trends in Production Engineering*, 1 (1), pp. 495-501. (doi:10.2478/ntpe-2018-0061)
40. Mrzljak, V. & Poljak, I. (2019) Energy Analysis of Main Propulsion Steam Turbine from Conventional LNG Carrier at Three Different Loads. *International Journal of Maritime Science & Technology "Our Sea"*, 66 (1), pp. 10-18. (doi:10.17818/NM/2019/1.2)
41. Mrzljak, V., Prpić-Oršić, J. & Poljak, I. (2018). Energy Power Losses and Efficiency of Low Power Steam Turbine for the Main Feed Water Pump Drive in the Marine Steam Propulsion System. *Journal of Maritime & Transportation Sciences*, 54 (1), pp. 37-51. (doi:10.18048/2018.54.03)
42. Orović, J., Mrzljak, V. & Poljak, I. (2018). Efficiency and Losses Analysis of Steam Air Heater from Marine Steam Propulsion Plant. *Energies*, 11, 3019. (doi:10.3390/en11113019)
43. Mrzljak, V., Anđelić, N., Poljak, I. & Orović, J. (2019). Thermodynamic analysis of marine steam power plant pressure reduction valves. *Journal of Maritime & Transportation Sciences*, 56 (1), pp. 9-30. (doi:10.18048/2019.56.01)
44. Mrzljak, V., Poljak, I. & Prpić-Oršić, J. (2019). Exergy analysis of the main propulsion steam turbine from marine propulsion plant. *Shipbuilding*, 70 (1), pp. 59-77. (doi:10.21278/brod70105)
45. Lemmon, E. W., Huber, M. L. & McLinden, M. O. (2010). *NIST reference fluid thermodynamic and transport properties – REFPROP*. Version 9.0. User's guide. NIST.
46. Cangioli, F., Chatterton, S., Pennacchi, P., Netti, L. & Ciuchicchi, L. (2018). Thermo-elasto bulk-flow model for labyrinth seals in steam turbines. *Tribology International*, 119, pp. 359-371. (doi:10.1016/j.triboint.2017.11.016)
47. Lorencin, I., Anđelić, N., Mrzljak, V. & Car, Z. (2019). Exergy analysis of marine steam turbine labyrinth (gland) seals. *Pomorstvo: Scientific journal of maritime research*, 33 (1), pp. 76-83, 2019. (doi:10.31217/p.33.1.8)
48. Blažević, S., Mrzljak, V., Anđelić, N. & Car, Z. (2019). Comparison of energy flow stream and isentropic method for steam turbine energy analysis. *Acta Polytechnica*, 59 (2), pp. 109-125. (doi:10.14311/AP.2019.59.0109)
49. Bishop, C. M. (2006). *Pattern Recognition and Machine Learning*. Springer.
50. Lorencin, I., Anđelić, N., Mrzljak, V. & Car, Z. (2019). Multilayer Perceptron approach to Condition-Based Maintenance of Marine CODLAG Propulsion System Components. *Pomorstvo: Scientific Journal of Maritime Research*, 33 (2), pp. 181-190. (doi:10.31217/p.33.2.8)

51. Lorencin, I., Anđelić, N., Mrzljak, V. & Car, Z. (2019). Marine Objects Recognition Using Convolutional Neural Networks. *International Journal of Maritime Science & Technology "Our Sea"*, 66 (3), pp. 112-119. (doi:10.17818/NM/2019/3.3)
52. Tuzikova, V., Tlustý, J. & Müller, Z. (2018). A novel power losses reduction method based on a particle swarm optimization algorithm using STATCOM. *Energies*, 11, 2851. (doi:10.3390/en11102851)
53. Lorencin, I., Anđelić, N., Mrzljak, V. & Car, Z. (2019). Genetic Algorithm Approach to Design of Multi-Layer Perceptron for Combined Cycle Power Plant Electrical Power Output Estimation. *Energies*, 12 (22), 4352. (doi:10.3390/en12224352)